World Academy of Science, Engineering and Technology
International Journal of Energy and Power Engineering
Vol:9, No:7, 2015

Near Shore Wave Manipulation for Electricity Generation

K. D. R. Jagath-Kumara, D. D. Dias

***Abstract*—**The sea waves carry thousands of GWs of power globally. Although there are a number of different approaches to harness offshore energy, they are likely to be expensive, practically challenging, and vulnerable to storms. Therefore, this paper considers using the near shore waves for generating mechanical and electrical power. It introduces two new approaches, the wave manipulation and using a variable duct turbine, for intercepting very wide wave fronts and coping with the fluctuations of the wave height and the sea level, respectively. The first approach effectively allows capturing much more energy yet with a much narrower turbine rotor. The second approach allows using a rotor with a smaller radius but captures energy of higher wave fronts at higher sea levels yet preventing it from totally submerging. To illustrate the effectiveness of the first approach, the paper contains a description and the simulation results of a scale model of a wave manipulator. Then, it includes the results of testing a physical model of the manipulator and a single duct, axial flow turbine in a wave flume in the laboratory. The paper also includes comparisons of theoretical predictions, simulation results, and wave flume tests with respect to the incident energy, loss in wave manipulation, minimal loss, brake torque, and the angular velocity.

***Keywords*—**Near-shore sea waves, Renewable energy, Wave energy conversion, Wave manipulation.

I. Introduction

THE use of water power dates back to thousands of years to the water wheels of Greece, Persia, and China, which used the energy of falling water to grind grain. However, the interest in harnessing energy from ocean surface waves began in France, the United States, and the UK in the 1800's. According to well established sources [1], [2] the potential of sea waves is enormous. In some offshore locations in both the hemispheres, the monthly average of the available wave power is as high as 200 kW/m [2]. However, the annual averages in the coastal areas range from about 5-50 kW/m [3]. There are at least 14 coastal regions in Sri Lanka, carrying a considerable amount of wave power. Here, in some months, the available power may range from 30-40 kW/m [3].

There is no doubt that the available energy of the sea waves at certain locations is adequate for a power plant of a useable scale. However, the fundamental problem is to harness this energy efficiently. There have been many different approaches used so far for generating electricity by using not only the surface waves but also the tidal waves in the sea. For example, a point absorber type wave energy converter with the dimensions in the order of 4–6.5 m can generate an annual average power of 86 kW when the annual available surface wave power is 38 kW/m [4]. In tidal flow, a wide bladed turbine having a diameter of 2.44 m has a total capacity of 45 kW at a flow velocity of 2.5 m/s, resulting in an overall efficiency of 57.1% [5]. The current cost of electricity generated using such approaches ranges from 0.07–0.10 $/kWh.

As the sea waves are available for free and are relatively reliable, the power plants using sea wave energy should be inexpensive needing only the cost of installation and maintenance. It is also an environmentally friendly approach for generating electricity. However, it appears that most of the current sea energy power plants are located offshore needing the expertise of professional seamen and high tech machinery for installation and maintenance. Therefore, it is useful to consider alternative approaches which are relatively inexpensive. This paper introduces new approaches for utilizing near-shore waves for generating electricity, reducing the installation and maintenance costs and, solving two fundamental problems associated with sea wave energy conversion. In addition, power plants using near shore waves would be less vulnerable to storms in the turbulent seas offshore, although the available energy is lower.

In this case, firstly, the near-shore wave fronts are funneled into a tunnel increasing the wave energy density [6]-[8]. The main advantage of this manipulation is that it enables to capture the energy of very wide waves, yet by using a turbine with dimensions in the order of some meters. After harnessing the wave energy inside the tunnel, the remaining waves are dispersed using a suitable diffuser. Secondly, a variable duct turbine (VDT) is used as a solution to the random variation of the wave height and the sea level. This paper mainly describes the simulation and testing of a scale model of such a wave manipulator and some trials with an existing type of a turbine.

Section II of this paper contains an overview of the various statistics of the sea waves. Section III briefly reviews the existing technologies used for utilizing the sea wave energy. Section IV describes the simulation and laboratory testing of the model manipulator. Then, it illustrates some results quantifying the wave parameters and the levels of energy density increase, and making comparisons to theoretical predictions. Section V introduces a variable duct turbine (VDT) suitable for random sea waves with random heights. Section V also presents test results obtained by mounting an existing type of a turbine inside the model manipulator. Section VI concludes the paper.

K. D. R. Jagath-Kumara is with the Department of Electrical and Electronic Engineering, University of Peradeniya, Peradeniya 20400, Sri Lanka (corresponding author to provide phone: +94-81-2393406; fax: +94-81-2385772; e-mail: jagathk@ ee.pdn.ac.lk).

D. D. Dias, is with the Department of Civil Engineering, University of Peradeniya, Peradeniya 20400, Sri Lanka (e-mail: daham@pdn.ac.lk).

II. Statistics of Sea Waves

The total wave power of all the oceans ranges up to a few thousands of GWs. For example, [1] contains a database of global wave statistics compiled using satellite altimeters since 1970's, visual observations carried out over 130 years, and instruments mounted on buoys rather recently. In addition, it also presents a corrected version of the visual data after some mathematical processing. According to all the three approaches, in the North Eastern Atlantic region, the mean significant wave height (H_s) ranges from just less than 1 m to 8 m with a peak probability of about 25% at 2.5 m height. Even 4 m high waves seem to occur at a probability of about 18%. In this case, H_s is the average height of the highest one third of the waves observed over a long enough time interval and the wave height is a combination of both the sea level height and the swell height. In an offshore location in India, the probability density function of H_s is more or less the same with a peak of 28% at a height of 2 m. The wave periods range from 5 to 12 s for both locations while the probability of occurrence of the period of 8.5 s is about 27%, which is the peak. The period here, is the zero crossing period.

The statistics of the available power in both the offshore and the near shore regions are given in [2]–[4]. These are too based on the measurements collected using buoys located at a large number of grid points in all the oceans, using various satellites, and using visual observations. In most cases, these data have been validated using mathematical modeling and comparison. Interestingly, the maximum annual average of the available wave power offshore is 140 kW/m at a location (48^0 S, 90^0 E), in the Southern hemisphere. This is 90 kW/m at (57^0 N, 21^0 W), in the Northern hemisphere. In January and July, the monthly averages reach a remarkably high figure of 200 kW/m, in both the hemispheres.

However, the annual averages of wave power in the coastal areas range from only 5 kW/m to 50 kW/m [3]. For example, the coastal areas in the countries near the equator averages between 15–20 kW/m of wave power. In the Northern hemisphere, the west coast of British Isles, Iceland, and Greenland and in the Southern hemisphere, Southern Chile, South Africa, the South and the South West of Australia and New Zealand provide the highest annual average [3]. Moreover, near shore wave heights and power have been predicted very precisely by using satellite data and buoys mounted near shore. According to these tests, the available power in the western coastal areas in Norway ranges from 29 – 36 kW/m.

A. Sea Wave Statistics in Sri Lanka

The Southern and the Western coastal regions of Sri Lanka receive promising 30-40 kW/m waves in July [3]. The lowest monthly average in these regions is 10–15 kW/m in January. The annual averages for Sri Lanka are 20–30 kW/m in the same regions and 5–10 kW/m in the eastern shore [4].

The surf forecast for Galle too, [9] provides more evidences on the wave energy generating capacity in the Southern seas of Sri Lanka. In June and July, 2–3 m high waves occur 80% of the time and this percentage reduces to 40% in May, August and September. The wind speed during these months is 20–30 km/h, 80% of the time, to which the wave velocity relates to. However, from December to March, 80% of the time, the wave heights range from only 0.5–1.3 m.

The energy forecast for Galle in December is about 80-158 kJ/m/wave when the average height and the period of the waves are 0.5–0.6 m and 12–14 s respectively. These figures indicate a power availability of about 7–11 kW/m, approximately resembling with the data in [2]–[4]. The December figures also imply the minimum power and energy availability during the year in Galle. On the positive side, on the 11^{th} of June 2015, the energy forecast for Galle is 957 KJ/m/wave with a period of 16 s and a height of 1.4 m, suggesting a power availability of about 60kW/m. However, the surf forecast suggests that the near shore statistics would be somewhat less.

B. Energy Conversion of Sea Waves

The previous sub sections presented only the available energy or power of sea waves in a given location. However, it is not possible to extract all of that in practice with existing power conversion mechanisms. For example, a point absorber type wave energy converter (WEC) with the dimensions of the order of 4–6.5 m has generated 751 MWh annually in the Western shore of Portugal where the annual incident wave power is 38 kW/m [4]. This corresponds to 85.7 kW of extracted annual average power from an area which is 4–6.5 m wide. A case study presented in [10] too validates a generating capacity of the same order. It indicates that the wave energy generated is 200 MWh/m annually when the incident wave power is 25 kW/m, the significant wave height is 1.5–4 m and the period is 10.5-13.5 s.

The degree of seasonal variation of the wave statistics is an important parameter, which determines the implementation complexity of a wave energy conversion system [3], [4]. If the ratio between the highest and the mean wave heights at a particular near shore location is high, the design cost of a wave energy power plant would be high because it would be necessary to consider a large range of values for a given design parameter such as the diameter of a suitable turbine, strength of the supporting structures, and the ratings of the electrical systems. For example, this ratio is about 10 for the northern hemisphere suggesting large seasonal fluctuations. However, for Sri Lankan coastal areas, the same ratio is about only 3. Additionally, the minimum monthly average of the available power with respect to the annual average is about 60 – 70% showing that the seasonal fluctuations are much smaller. Therefore, the design complexity and the construction cost of a near shore wave power plant are comparatively smaller in Sri Lanka. This is also true for those countries near the equator and the Southern hemisphere.

In commenting on the cost, a study carried out in Australia [11] suggests a cost of \$100/MWh or 0.10 \$/kWh for sea wave energy. A case study in Tenerife, Spain discusses the effects of a wave farm on the near shore wave climate [12].

III. A Review of Existing Approaches of Harnessing Sea Energy

There are mainly two types of devices which are used for harnessing sea energy. The non-rotating wave energy converters (WECs) are used for converting mainly the potential energy of the surface waves in the sea. However, the rotating devices such as turbines are mainly used for extracting the kinetic energy of tidal flows and are installed under water.

A. WECs

Most of the WECs utilize the motion of two or more bodies relative to each other. One of these bodies, referred to as the displacer, is acted upon by the waves. The second body, referred to as the reactor, moves in response to the displacer [13]-[15]. They essentially convert the potential energy corresponding to the change in the wave height and the sea level height. For sinusoidal waves, the available potential energy per wavelength [16],

$$E_p = 0.25\rho g\lambda w a^2; \quad \text{if } a << \lambda \tag{1}$$

where ρ = density of water, g = gravitational acceleration, λ = wave length, w = width of the wave, and a = wave amplitude. Therefore, E_p is the maximum possible energy, a given WEC can harness per wavelength of the wave environment.

There are, broadly, four groups of WECs, known as point absorbers, attenuators, terminators, and overtopping devices. The working principles of these groups are clearly illustrated in [17]. A description of practical implementations, costs, and limitations are discussed in [13], [15].

1) Point Absorbers

This type of WECs utilizes the vertical movement of the waves to act as a pump. In one type, a floating buoy anchored to the sea floor with the turbine device as part of the vertical connection, moves up and down with the waves. This produces pumping action which drives the turbine. A point absorber type WEC described in [13] has a rated capacity of 250 kW. A 10 MW power station would require 40 of them installed in an area of 16 acres in 30 – 50 m deep water, about 1.6 to 8 km offshore. Although, the current costs are at 0.07 – 0.10 $/kWh, the future cost prediction is 0.03 – 0.04 $/kWh.

2) Attenuators

This type of a device effectively attenuates the rise of the wave height by the buoyancy and the weight of itself, resulting in energy transfer into the device. An implementation, which is known as Pelamis Sea Snake, consists of several floating segments jointed together. It is anchored to the sea floor at the two last segments and aligned towards the wave direction. The segments move up and down with the waves causing the joints to operate a turbine. A 140 m long, 3.5 m in diameter, four segment device with three joints, each connected to a 250 kW power conversion unit has a total power rating of 750 kW [13]. Such a unit is typically installed in 50–70 m deep water about 3–24 km offshore. A 30 MW power station would span 250 acres of sea area.

3) Terminators

A practical implementation of a terminator type device is known as the oscillating water column (OWC) WEC. The waves enter into a partially submerged collector from below. The change in water level changes the pressure of the trapped air at the top of the collector, causing a turbine to generate mechanical energy and then the electrical energy. A 1 MW demonstrative installation of this kind of a power station is 21 m wide and 24 m long, and has cost $8 M [18].

4) Over Topping Devices

This kind of devices uses the rise in wave height to obtain high head water. For example, a floating reservoir built in the ocean is filled when the waves break over the walls of it. The water level in the reservoir is made higher than that of the surrounding ocean surface realizing an adequate pressure head for a hydro turbine. The projected cost for a 4–11 MW power station is 0.04 €/kWh [13].

B. Hydrokinetic Energy Conversion

The waves propagate with a certain phase velocity transporting the energy at the corresponding group velocity. However, in the case of sea waves, the randomness of the wavelength, wave height, wave period, wave shape, and the wind make those velocities random too. On the other hand, tidal flows are more predictable and uniform with a rather steady velocity. It is also most common to use the kinetic energy of tidal flows for power extraction. In this case, a suitable turbine converts the kinetic energy of the tidal flow to mechanical energy, which drives an electrical generator. The available energy per meter of flowing water,

$$E_f = 0.5\rho A v^2 \tag{2}$$

where A = area of the water column normal to the direction of flow and v = velocity of flow. This implies that the maximum energy, a hydrokinetic turbine can extract is E_f. Then, the mechanical power, a given turbine extracts is,

$$P_m = C_p(E_f v) = 0.5C_p\rho A v^3 \tag{3}$$

where C_p is the power coefficient which indicates how efficient the turbine is in capturing energy. Therefore, the amount of electrical power, a certain generator coupled to this turbine generates is,

$$P_e = 0.5C_eC_p\rho A v^3 \tag{4}$$

where C_e is the efficiency of the generator.

There are two types of hydrokinetic turbines known as impulse turbines and free-flow turbines.

1) Impulse Turbines

In this case, a suitable device first converts the pressure head of the water kept in a reservoir into a high speed jet. The jet of water then impinges on the blades of an appropriate rotor resulting in rotations. A typical example is Pelton-wheel turbine which can reach an efficiency (water to turbine shaft) of 100% when the tangential velocity of the tips of the blades is half of the velocity of the water-jet. In a practical implementation, a Pelton-wheel turbine generated about 45 MW with a 114 m/s jet resulting in a volumetric flow of 7 m^3/s [19]. This set the rotor velocity to be 56 m/s which was slightly below half of that of the jet.

2) Free-flow Turbines

There is a variety of free-flow turbines which extract the kinetic energy of tidal flows. For example,

a) Horizontal axis turbines: With horizontal axis turbines, the water flows parallel to the axis of the turbine and impinges on the plain of the rotation. The propeller type, whose blades are narrow and have the shape of an aerofoil, depends on the lift force on each blade whereas the fan blade type with wide blades seems to use the reactive force as well as the impulsive force.

According to the theoretical predictions and simulations, these devices have an efficiency of about 50% at a tip-speed-ratio (TSR) of about 2, which is the ratio of the tangential velocity of the tip of the rotor and the flow velocity. The typical velocity of tidal flows is in the range of 1 to 3 m/s resulting in an extracted power of close to 1 MW.

A propeller type turbine with a diameter of 5 m can generate 35 kW at a tidal flow of 2 m/s [20]. An array of 30 such turbines would realize a 1 MW power station. It would cost 2500 $/kW for a 5 MW power station with propeller type tidal turbines. A wide bladed twin-turbine having a diameter of 2.44 m each, has a total capacity of 90 kW at a flow velocity of 2.5 m/s, resulting in an overall efficiency of 57.1%. A similar twin-turbine, each with a diameter of 3.048 m, would yield 600 kW at 4 m/s [5].

b) Vertical axis turbines: In these turbines, the blades are vertically mounted around the shaft, which too is vertical, using horizontal struts. Therefore the water flows in a perpendicular direction to the axis of the turbine. For example, the blades of Darrieus turbine have a uniform aerofoil-shaped cross section resulting in a maximum efficiency of 43% at a specific TSR which is close to 3.5 [21]. Over the velocity range of 1 to 3 m/s, it has reached an efficiency of 35% in a practical implementation. In some instances, Darrieus turbine has extracted some hundreds of kilowatts.

c) Golov turbine: This type, which is also known as the helical turbine, is somewhat similar to Darrieus turbine but the blades are not vertical and straight due to twisting. It has an efficiency of about 25% at a TSR of about 2, in the velocity range of 1 to 3 m/s. However, the efficiency could reach 35% according to theoretical predictions. Golov turbine can function in both the horizontal axis and the vertical axis modes. Some report that by cascading several of these rotors, it is possible to intercept very wide flows. In 2009 [22], two Golov turbines with a total rating of 1 MW were installed in tidal flow commercially.

d) Water-wheel: This oldest version of the water turbine has rectangular blades each of which is connected to two struts. The struts are in turn connected to a hub. This is a horizontal axis turbine and the axis is perpendicular to the direction of flow. Normally, less than 50% of the wheel is immersed in the water while the rest is over the surface of the water [23].

IV. Near Shore Energy Manipulation

As described in Section II, the available energy and the power of a certain wave is proportional to the width, w. For example, for near shore locations, the annual average of the available power ranges from 5 to 50 kW/m [3]. Therefore, any electro-mechanical system which utilizes near shore wave energy must have the dimensions of the order of 100 meters, in order to generate a few MWs of power. This sets a practical limit to any attempts to utilize wave energy for generating mechanical or electrical power. As a solution, this paper proposes to manipulate the waves increasing the energy density.

Fig. 1 shows a schematic of a near shore structure which would funnel, tunnel and diffuse the waves [6]–[8]. The funnel section concentrates very wide (w_1) waves into narrow waves (w_2), where $w_1 >> w_2$. The tunnel allows these narrow waves to stabilize, for example, with respect to the direction of the movement, wave length, velocity and the frequency. After this manipulation, the wave length and then the wave velocity must increase inside the tunnel increasing the energy density. In other words, a square meter of waves inside the tunnel carries much more energy than the original waves do. Once, an appropriate electro-mechanical assembly converts this energy, the diffuser, which inverses the funneling function, is to disperse the remaining power of the waves without flooding the shore considerably. In Fig. 1, b_1, b_2, and b_3 are the lengths of the corresponding sections, α and β are the funneling and diffusing angles, and w_3 is the width of the diffuser exit.

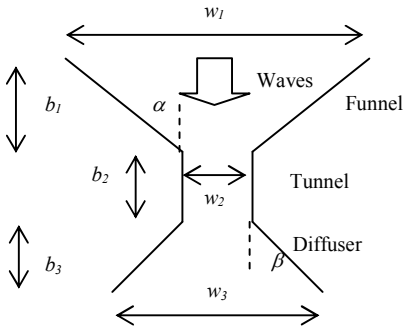

Fig. 1 Funneling, tunneling and diffusion

Theoretical research presented in the literature suggests that the wave length and the height of sinusoidal waves increase when the width of the channel decreases, which ascertains the

effectiveness of this approach. For example, [24] shows mathematically, that the wavelength should increase if the width (w) of the channel decreases. By experimentally and numerically [25] shows that the amplitudes of waves should increase in proportional to $w^{-0.5}$ in a converging channel and should decrease in proportional to $w^{-0.66}$ in a diverging channel. Note that in [25] one of the walls of the channel is straight whereas the other one is slanting forward.

The effectiveness of the wave manipulation process could be quantified by the ratio of the amount of energy per meter of width at the funnel entrance and that in the tunnel. If the incident wave is sinusoidal, the kinetic energy per wave length [16],

$$E = 0.25\rho g\lambda w a^2;\ a << \lambda \tag{5}$$

and that per unit width,

$$e = \frac{E}{w} = 0.25\rho g\lambda a^2. \tag{6}$$

(Note that the total energy in the wave is twice as much with an equal amount of potential energy.) Then, the coefficient of energy density increase,

$$c_{edi}^{\sin} = \frac{e_2}{e_1} = \frac{0.25\rho g\lambda_2 {a_2}^2}{0.25\rho g\lambda_1 {a_1}^2} \tag{7}$$

where the suffixes of 1 and 2 represents the corresponding parameters of the incident wave and the wave in the tunnel respectively. For a fully enclosed tunnel, where $a_2 = a_1$,

$$c_{edi}^{\sin} = \frac{\lambda_2}{\lambda_1}. \tag{8}$$

Since, λ is approximately proportional to the wave velocity, v [16],

$$c_{edi}^{\sin} = \frac{\lambda_2}{\lambda_1} \approx \frac{v_2}{v_1}. \tag{9}$$

If the wave manipulator has a constant height, the conservation of mass yields

$$\rho w_1 v_1 = \rho w_2 v_2. \tag{10}$$

By combining (9) and (10),

$$c_{edi}^{\sin} \approx \frac{w_1}{w_2} \tag{11}$$

where $\frac{w_1}{w_2}$ is the funneling ratio. According to (9) and (11) the effectiveness of the process directly corresponds to the increase in wave length, increase in velocity or the funneling ratio.

However, the sea waves near shore do not appear to be sinusoidal. Their cross section almost resembles the shape of a triangle with smooth edges. When the waves break, it more or less resembles the raised cosine shape. In addition, such wave shapes and the corresponding periods change randomly from time to time. To be very precise, it is possible to decompose them into constituent sinusoidal waves and estimate the statistical averages of energy and power using the wave parameters collected over a long time [1]–[4].

On the other hand, for a steady triangular wave sequence of the form illustrated in Fig. 2, the momentum theory can yield the energy per wave. Note that Fig. 2 is an approximation of the sea waves according to visual observations. Then, the kinetic energy carried in such a wave crest,

$$E = 0.25\rho bhwv^2 \tag{12}$$

where w is the width and s is the distance between two successive crests.

From (12), the energy density per unit width,

$$e = \frac{E}{w} = 0.25\rho bhv^2. \tag{13}$$

Then, the effectiveness of the energy density increase in the manipulation process is given by the coefficient,

$$c_{edi}^{sea} = \frac{e_2}{e_1} = \frac{b_2 h_2 {v_2}^2}{b_1 h_1 {v_1}^2} \approx \frac{w_1}{w_2}. \tag{14}$$

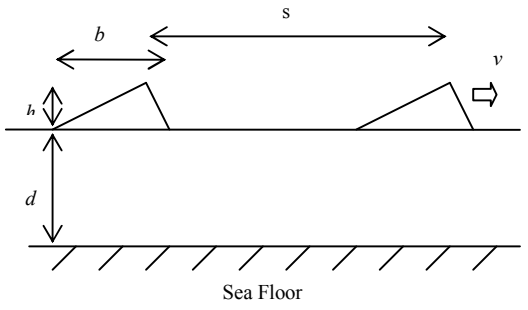

Fig. 2 An approximate wave sequence

In (14) too, the suffixes of 1 and 2 represent the corresponding parameters of the incident wave and the wave in the tunnel respectively. This implies that the effectiveness of the wave manipulation, with respect to the energy per unit width, is equal to the funneling ratio for a given sea wave too.

In (9), (11), and (14), the loss in the wave manipulation process due to reflections and eddies, has not been considered. Therefore, e_2 should be substituted with (e_2-l), where l is the corresponding loss per unit width. It will be shown in the results section that this loss is small for reasonable values of the funneling ratios. Hence, (9), (11), and (14) are good

indicators of the effectiveness of the wave manipulation process.

A. A Model of a Wave Manipulator

To test the applicability and the predicted effectiveness of wave manipulation, it is first necessary to build a scale model. This should also help estimating the optimal dimensions which are w_1, w_2, w_3, b_1, b_2, and b_3. These results can then predict the size and the power generation capacity of a real prototype under given wave conditions.

TABLE I
SIMULATION RESULTS FOR w_2=0.25 m

α	w_1 (mm)	h_2 (m)	λ_2 (m)
30^0	750	0.34	2.4
45^0	957	0.38	2.5

TABLE II
SIMULATION RESULTS FOR w_2=0.35 m

α	w_1 (mm)	h_2 (m)	λ_2 (m)
30^0	850	0.38	2.20
45^0	1057	0.42	2.45

TABLE III
SIMULATION RESULTS FOR w_2=0.45 m

α	w_1 (mm)	h_2 (m)	λ_2 (m)
30^0	950	0.38	2.05
45^0	1157	0.40	2.25

For example, if $\frac{w_1}{w_2}$ is too high, the level of energy density increase will be smaller than expected due to the increase in losses. Particularly, if w_2 is very small, a stagnation point occurs close to the tunnel entrance and the volumetric flow through the tunnel may become very small too. For a given w_1, when $\frac{w_1}{w_2}$ decreases, the losses too decrease increasing the velocity and the volumetric flow. If $\frac{w_1}{w_2}$ decreases further, the level of wave manipulation becomes lower and the velocity (wave length) starts to decrease. In this way, the losses become smallest possible for no concentration ($\frac{w_1}{w_2}=1$) caused by only the surface resistance of the walls with no velocity (or energy density) increase. Therefore, for a given w_1, the model should enable to estimate the smallest tunnel width, $w_{2,opt}$, for which the losses are minimal and close to those of no manipulation. In other words, this w_1 and $w_{2,opt}$ should increase the velocity by keeping the volumetric flow and the energy as close as possible to that of the original waves captured by the funnel section effectively providing the highest energy density increase. The tunnel width, $w_{2,opt}$, is then the major dimension of the turbine.

The scale model of the manipulator was constructed using Aluminum for minimizing frictional losses and enhancing the durability. The length of the tunnel (b_2) was 2 m. The tunnel width (w_2) could be adjusted by sliding the walls of it. The funnel and the diffuser, each 0.5 m long, were joined to the tunnel by using hinges so that w_1 and w_3 as well as b_1 and b_3 could be changed. All the three sections had a constant height of 1.2 m.

B. Simulation Using Delft3D

The use of computational fluid dynamics (CFD) to analyze and predict the dynamics of the near shore coastal environment has increased considerably during the past decades. With CFD, process oriented numerical models which are based on the basic physical equations such as mass and momentum conservations facilitate near shore wave related studies. They incorporate numerous processes which take place in the near-shore environment, such as the wave movements, wind effects, and the subsequent alterations of wave trains due to manipulations. Further, the model users have the facility of idealizing the model depending on the requirements, isolating the pivotal processes which influence the final wave parameters.

Delft3D [26] is a modular open source code developed by Deltares, and provides an integrated framework for a multi-disciplinary approach, creating 2D and 3D computer simulations of waves and tides in the coastal areas. In this case, the wave manipulator was represented as a spatial obstacle which has been placed in a domain with the dimensions of the laboratory wave flume using "WAVE" section of the Delft3D. No wave propagation was allowed outside this domain in the simulation. The grid and bathymetry files were developed and incorporated into the simulation with the basic data. The time frame and the boundary conditions for the analysis were selected to be adhered with the study. The effect of the local winds was neglected due to the inability of generating wind when performing the laboratory model tests.

The simulation was performed for different angles of the funnel (α), that of the diffuser (β), and for different tunnel widths (w_2) with a sinusoidal incident wave having a wavelength (λ_1) of 1.3 m, height (h_1) of 0.34 m, and a period (T_1) of 1.2 s. The width of the funnel entrance (w_1) was effectively changed when α was changed. The simulation data was processed using MatLab to obtain the wave parameters in the manipulator.

According to the simulations, for a given w_1, h_2 and λ_2 are initially smaller for smaller values of w_2 because the water flow stagnates at the tunnel entrance. When w_2 increases to about 0.25 m, h_2 and λ_2 also increase indicating the enhancement of the energy density. If w_2 is too large (about 0.5 m) causing $\frac{w_1}{w_2}$ to be too small, h_2 and λ_2 again starts decreasing, due to the lower level of wave manipulation. For example, Tables I to III show the wave parameters in the tunnel obtained through the simulations for w_2 = 0.25 m, 0.35 m, and 0.45 m, $\alpha = 30^0$ and 45^0, and $\beta = 45^0$.

Tables IV-VI show the kinetic energy of the incident wave (E_1), that in the tunnel (E_2), and the energy loss ($L=E_1-E_2$) in Joules calculated from (5) using the simulation data in Tables

I-III respectively. These tables also list the corresponding energy densities (e_1 and e_2), which are the amounts of energy per unit width of the wave (in Joules per meter) and $c_{edi}^{\sin}$ which is ($\frac{e_2}{e_1}$).

TABLE IV
KINETIC ENERGY DENSITY FOR w_2=0.25 m (SIMULATIONS)

w_1/w_2	α	E_1 (J)	E_2 (J)	L (J)	e_1 (J/m)	e_2 (J/m)	$c_{edi}^{\sin}$
3.0	30^0	69	43	26	92	170	1.8
3.8	45^0	88	56	32	92	222	2.4

TABLE V
KINETIC ENERGY DENSITY FOR w_2=0.35 m (SIMULATIONS)

w_1/w_2	α	E_1 (J)	E_2 (J)	L (J)	e_1 (J/m)	e_2 (J/m)	$c_{edi}^{\sin}$
2.4	30^0	79	68	11	92	195	2.1
3.0	45^0	98	93	5	92	265	2.9

TABLE VI
KINETIC ENERGY DENSITY FOR w_2=0.45 m (SIMULATIONS)

w_1/w_2	α	E_1 (J)	E_2 (J)	L (J)	e_1 (J/m)	e_2 (J/m)	$c_{edi}^{\sin}$
2.1	30^0	88	82	6	92	182	2.0
2.6	45^0	107	100	7	92	221	2.4

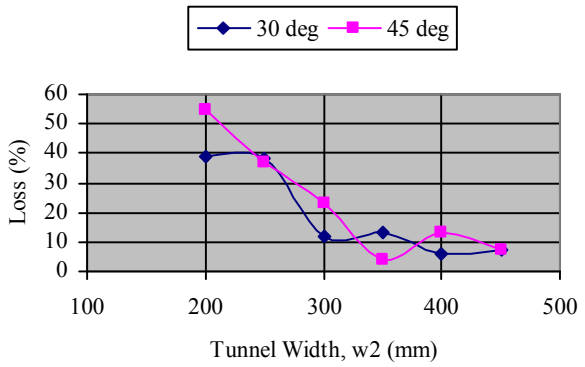

Fig. 3 Percentage loss in wave manipulation for $\alpha = 30^0$ and 45^0

According to energy density calculations, $c_{edi}^{\sin}$ is very close to $\frac{w_1}{w_2}$ as predicted by (11) except for small w_2 (less than 0.25 m), due to the stagnation. It has been further observed that $c_{edi}^{\sin}$ deviates significantly for $\alpha > 45^0$. This is because, when α is high, the incident wave reflects off the walls of the funnel opposing the oncoming waves rather than directing them into the tunnel.

Fig. 3 shows the energy loss in the wave manipulation process as a percentage of the energy of the incident wave, which is $\frac{L}{E_1}\times 100$, for different tunnel widths (w_2). According to this representation of simulation results, the percentage loss seems to approach a minimum of about 10 when w_2 is high. The smallest w_2 which result in a loss close to this minimum loss are 0.3 m and 0.35 m for $\alpha = 30^0$ and 45^0 respectively. Further, w_2 = 0.35 m at $\alpha = 45^0$ provides the highest kinetic energy density of 265 J/m in the tunnel with $c_{edi}^{\sin}$ of 2.9 and hence is the best choice considering these set of simulations. However, in order to estimate the optimum tunnel width ($w_{2,opt}$), it is a good practice to carry out more simulations and preferably more laboratory model tests, covering higher values of $\frac{w_1}{w_2}$ and with a higher resolution of w_2.

For comparison, the sinusoidal incident waves can be approximated to the triangular waves of the form in Fig. 2 and the kinetic energy could be estimated using the momentum theory as given in (12) and (13). Further, the corresponding group velocity (v) too needs to be approximated using the wave theory. In this case, for the incident wave, $d > \lambda/2$ where d = 1.2 m and λ = 1.3 m, allowing to use the deep water assumption. Hence, the group velocity is given by [16],

$$v = \frac{gT}{4\pi}. \tag{15}$$

For the tunnel section, this is given by [16],

$$v = \frac{c}{2}\left[1+\frac{4\pi d}{\lambda}\frac{1}{\sinh\left(\frac{4\pi d}{\lambda}\right)}\right] \tag{16}$$

where λ is a few times d.

In (16),

$$c = \sqrt{\frac{g\lambda}{2\pi}\tanh\left(\frac{2\pi d}{\lambda}\right)} \tag{17}$$

which is the phase velocity.

For w_2 = 0.25 m and 0.45 m, the quantities of interest evaluated by using (12) – (17) are listed in Tables VII and VIII respectively.

TABLE VII
KINETIC ENERGY DENSITY FOR W_2=0.25 m (SIMULATIONS) (FROM (12) – (17))

w_1/w_2	α	E_1 (J)	E_2 (J)	L (J)	e_1 (J/m)	e_2 (J/m)	$c_{edi}^{\sin}$
3.0	30^0	73	50	23	97	199	2.1
3.8	45^0	93	61	32	97	244	2.5

TABLE VIII
KINETIC ENERGY DENSITY FOR W_2=0.45 m (SIMULATIONS) (FROM (12) – (17))

w_1/w_2	α	E_1 (J)	E_2 (J)	L (J)	e_1 (J/m)	e_2 (J/m)	$c_{edi}^{\sin}$
2.1	30^0	92	71	21	97	159	1.6
2.6	45^0	112	92	20	97	204	2.1

It can be seen that the values in Tables IV and VI are somewhat close to those in Tables VII and VIII respectively, reasonably justifying the validity of (12) and (13).

C. Testing in the Wave Flume

The physical scale model was partially submerged in the large wave flume which is 30 m long, 1.8 m wide, and 2.1 m deep, and consists of smooth concrete walls, as illustrated in Fig. 4. In order to avoid the effect of reflecting waves, it was located a reasonable distance away from the wave breaker at the end of the flume. The level of the still water was kept at 1.2 m. With the plunger type wave maker, the same sinusoidal incident wave used for the simulations was generated for testing. The measured wave parameters in the tunnel are given in Tables IX and X.

Fig. 4 Photograph of the model manipulator in the flume

TABLE IX
MEASURED PARAMETERS FOR w_2=0.25 m (TESTING)

α	w_1 (mm)	h_2 (m)	λ_2 (m)
30^0	670	0.38	2.7
45^0	957	0.45	2.6

TABLE X
MEASURED PARAMETERS FOR w_2=0.45 m (TESTING)

α	w_1 (mm)	h_2 (m)	λ_2 (m)
30^0	860	0.39	1.8

TABLE XI
KINETIC ENERGY DENSITY FOR w_2=0.25 m (TESTING)

w_1/w_2	α	E_1 (J)	E_2 (J)	L (J)	e_1 (J/m)	e_2 (J/m)	$c_{edi}^{\sin}$
2.7	30^0	62	60	2	92	238	2.6
3.8	45^0	88	81	7	92	322	3.5

TABLE XII
KINETIC ENERGY DENSITY FOR w_2=0.25 m (TESTING)

w_1/w_2	α	E_1 (J)	E_2 (J)	L (J)	e_1 (J/m)	e_2 (J/m)	$c_{edi}^{\sin}$
1.9	30^0	79	76	3	92	168	1.8

TABLE XIII
KINETIC ENERGY DENSITIES FOR w_2=0.25 m (TESTING) (FROM (12) – (17))

w_1/w_2	α	e_1 (J/m)	e_2 (J/m)	$c_{edi}^{\sin}$
2.7	30^0	97	291	3.0
3.8	45^0	97	316	3.3

TABLE XIV
KINETIC ENERGY DENSITIES FOR w_2=0.45 m (TESTING) (FROM (12) – (17))

w_1/w_2	α	e_1 (J/m)	e_2 (J/m)	$c_{edi}^{\sin}$
1.9	30^0	97	124	1.3

Again, the kinetic energy of the incident wave (E_1) and that in the tunnel (E_2) were calculated from (5) using the data in Tables IX and X. Tables XI and XII include those energies (E_1 and E_2), the energy losses (L) in the concentration, and the energy densities (e_1 and e_2). They also show the corresponding $c_{edi}^{\sin}$. Thus, estimations based on the laboratory test results confirm that $c_{edi}^{\sin}$ is very close to $\frac{w_1}{w_2}$ as in (11), for these two selected values of w_2. Further, the percentage loss in the energy concentration process is less than 10%. Note that the laboratory model test results more closely approximate the theoretical predictions than the simulation results do, due to non-incorporation of all the wave processes in the CFD simulations.

In these cases, the free movement of the waves in the tunnel, which was kept open for taking measurements, allowed not only the wave velocity but also the wave height to rise. Therefore, the velocity increase is not as high as that implied in (10). The increase in energy density in the tunnel is caused by the corresponding increases in both the velocity and the height of the wave, with these tests.

For comparison, Tables XIII and XIV list the energy densities and the coefficients of energy density increase evaluated by approximating the sinusoidal waves to triangular waves and by using (12)–(17). In this case, although the incident energy densities are close to those in Tables XI and XII, there are some deviations in those in the tunnel.

V. A Suitable Turbine for the Enhanced Near Shore Waves

Once the sea waves are manipulated to increase the kinetic energy density, the resulting flow is somewhat similar to that of a jet and also that of a free flow. It is impulsive periodically (corresponding to the original wave crests) with a fluctuating volumetric flow rate. Therefore, both the impulse turbines and free-flow turbines [13]–[15] could be more suitable for this application. In particular, the Pelton-wheel, the water-wheel, or a combination of them may be the best type of turbine.

A. A Variable Duct Turbine (VDT)

According to the preceding paragraph, the most efficient type of the turbine could be similar to the horizontal axis Pelton-wheel, however with wider, curved blades allowing them to intercept broader flows as well as to capture impulsive forces. Fig. 5 illustrates the cross section of such a rotor. In this case, the width of the rotor is the optimum tunnel width ($w_{2,opt}$) but the radius is a question due to the statistical nature of wave parameters.

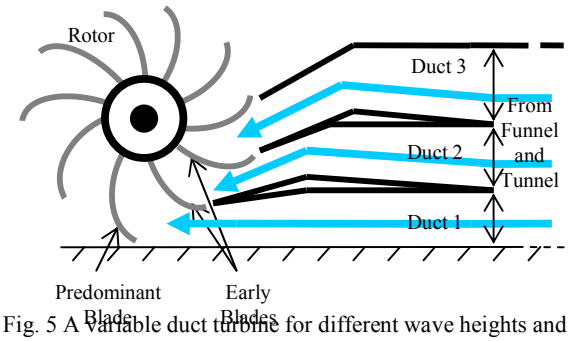

Fig. 5 A variable duct turbine for different wave heights and sea levels

In this case, the sea level, wave height, wave length, frequency, and the velocity fluctuate randomly causing the available power to fluctuate accordingly. One of the main problems is to adjust the rotor radius (blade length) so that it intercepts the full cross section of the prevailing waves and extracts the total available power. If the rotor radius is highest possible (which is equal to the tunnel height, in this case), it may stall due to the high inertia whenever the wave height (wave power) becomes small. On the other hand, if the rotor is too small compared to the size of the tunnel, it would completely immerse in water and would still stall due to the opposing force acting on the top side blades. Therefore, this paper also introduces a variable duct turbine (VDT) as a solution to the fluctuating sea levels. With VDT, the rotor radius is equal to the most frequent wave height and it does not expose itself directly to any higher waves as illustrated in Fig. 5. Instead, a set of ducts guide the wave fronts, which are higher than the most frequent, so that they impinge on the appropriate early blades only. The early blades are those which always aid the rotation in the same direction. Although, a suitable model is yet to be constructed, the main design considerations are described next. Fig. 5 shows how ducting manipulates varying wave levels to drive multiple blades of a Pelton-wheel type turbine. Note that the dimensions of Duct 1 are such that it acquires most frequent waves which exerts power on the predominant blade. Therefore, the blade length and then the rotor size are smaller than the height of the highest wave possible (height of the tunnel). Therefore, smaller wave fronts in Duct 1 can still rotate it due to lower moment of inertia. Note that the height of the most frequent wave determines the blade length of the rotor. If the wave fronts are any higher than the most frequent type, Duct 2 and Duct 3, in order, guide them so that they impinge on the corresponding early blades. In designing the rotor, the number of ducts must be made suitable to the expected range of variation of wave heights, omitting the very small waves carrying no significant power and the very large waves which are infrequent. Then, the number of ducts, in turn, determines the number of early blades and the total number of blades. However, too narrow ducts attenuate the waves causing loss of wave power. An optimum number of ducts which are broad enough, results in a higher efficiency of power extraction in random seas.

B. Testing the Manipulator with a Model of a Turbine

The axial flow, horizontal axis turbines with wide blades (fan type) has an efficiency which is close to 50% in free flow channels according to the literature [5], [13]. Therefore, two fan blade type horizontal axis turbines with the diameters of D_1=0.18 m and D_2=0.38 m were assembled for this purpose. First, the smaller one was installed at the end of the tunnel by keeping w_2=0.25 m as illustrated in Fig. 6. For the same incident wave described in Section IV, the brake torque (τ) and the angular velocity (ω) were measured. These measured values for $\alpha = 30^0$ and 45^0 are listed in Table XV. Then, the procedure was repeated with the 0.38 m turbine by setting w_2 to 0.45 m. The measured values for $\alpha = 30^0$ are listed in Table XVI.

Fig. 6 Turbine placed at the tunnel end

Note that the 0.18 m turbine intercepted only a part of the available energy because the wave heights for this case was 0.38 m and 0.45 m for $\alpha = 30^0$ and 45^0 respectively. Otherwise, the brake torque and the angular velocity could have been much higher. However, the 0.38 m turbine could capture most of the energy of 0.39 m high waves in the tunnel. This increased the brake torque by a factor of about 12.

VI. Conclusion

A near shore wave energy manipulator for electricity generation was proposed and analyzed theoretically considering the sinusoidal waves and an approximated version of sea waves. The parameters corresponding to the effectiveness of a model manipulator were found using CFD simulations and wave flume tests. Simulations suggested that the coefficient of energy density increase is similar to the funneling ratio for tunnel widths which are not too small. These simulation results helped in estimating the minimum tunnel width for which the manipulation loss is close to that of no manipulation.

TABLE XV
TURBINE MEASUREMENTS (D_1=0.18 m)

α	w_1 (m)	w_1/w_2	τ (Nm)	ω (rpm)
30^0	670	2.7	1.3	1205
45^0	957	3.8	1.5	833

TABLE XVI
TURBINE MEASUREMENTS (D_2=0.38 m)

α	w_1 (m)	w_1/w_2	τ (Nm)	ω (rpm)
30^0	860	1.9	15.6	-

The coefficients of energy density increase, obtained by testing the scale model in the wave flume, better agreed with the theory in approximating the funneling ratio. These results also helped in determining the optimum tunnel width and the funneling ratio. The tests with the axial flow, horizontal axis turbines, suggested the level of energy density increase realized by the wave manipulation. It is necessary to carry out more simulations and tests for different kinds of incident waves and for higher funneling ratios.

The major design parameters of a variable duct turbine suitable for fluctuating sea levels and wave heights were described. Such a turbine will be constructed for testing in the future.

ACKNOWLEDGMENT

We acknowledge the support received from the staff of the workshops of the Departments of Production and Electrical Engineering, Faculty of Engineering, University of Peradeniya. We are also grateful to the staff of the Fluid Mechanics Laboratory and the final year project students of the same faculty, who were involved in this project. This project has received funds from Tokyo Cement Research Fund.

REFERENCES

[1] Global wave statistics, BMT fluid mechanics Limited, http://www.globalwavestatistics.com/Help/comparison.htm/, 2011.
[2] Ocean wave climate, Fugro OCEANOR, http://www.oceanor.com/, 2014.
[3] S. Barstow, G. Mørk, L. Lønseth, J. P. Mathisen, "WorldWaves wave energy resource assessments from the deep ocean to the coast," in *Proc. 8th European Wave and Tidal Energy Conf.*, Uppsala, Sweden, 2009, pp. 149-159.
[4] G. Mørk, S. Barstow, A. Kabuth, M. T. Pontes, "Assessing the global wave energy potential," in *Proc. 29th International Conf. on Ocean, Offshore Mechanics and Arctic Engineering (OMAE)*, Shanghai, China., 2010.
[5] http://uekus.com/.
[6] B. Thanatheepan, S. Gobinath, K. D. R. Jagath Kumara., "A case study on near shore wave energy utilization in the coastal regions of Sri Lanka," in *Proc. National Energy symposium 2013*, BMICH, Colombo, Sri Lanka, 2013, pp. 56-71.
[7] S. D. K. Maliyadda, W. M. C. R. Wijeratne, S. R. L. M. Zoysa, D. D. Dias, K. D. R. Jagath-Kumara, "Wave manipulation for near shore wave energy utilization," in *Proc. National Energy Symposium*, BMICH, Colombo, Sri Lanka, 2014, pp. 94-104.
[8] S. D. K. Maliyadda, W. M. C. R. Wijeratne, S. R. L. M. Zoysa, D. D. Dias, K. D. R. Jagath-Kumara, "Manipulation of near-shore sea waves for electricity generation: modelling a wave concentrator," in *Proc. 5th International Conference on Sustainable Built Environment, ICSBE 2014*, Kandy, Sri Lanka, vol. 3, 2014, pp. 206-216.
[9] Galle surf and wind quality by month (West, Sri Lanka), http://www.surf-forecast.com/, 2014.
[10] G. Iglesias, R. Carballo, "Wave energy and near-shore hot spots: The case of the SE bay of Biscay," *Renewable Energy*, vol. 35, issue 11, pp. 2490-2500, Nov. 2010.
[11] J. Morim, N. Cartwright, A. Etemad-Shahidi, D. Strauss, M. Hemer, "A review of wave energy estimates for nearshore shelf waters of Australia," *International Journal of Marine Energy*, vol. 7, pp. 57-70, Sept. 2014.
[12] M. Veigas, V. Ramos, G. Iglesias, "A wave farm for an island: Detailed effects on the nearshore wave climate," *Energy*, vol. 69, pp. 801-812, May 2014.
[13] *Proceedings of the Hydrokinetic and Wave Energy Technologies*, Technology and Environmental Issues Workshop, Washington D. C., 26 – 28 Oct. 2005.
[14] M. J. Khan, G. Bhuyan, M. T. Iqbal, J. E. Quaicoe, "Hydrokinetic energy conversion systems and assessment of horizontal and vertical axis turbines for river and tidal applications: A technology status review," *Elsevier Journal of Applied Energy*, vol. 86, issue 10, pp. 1823-1835, 2009.
[15] S. L. Ortega-Achury, W. H. McAnally, T. E. Davis, J. L. Martin, "Hydrokinetic Power Review," Civil and Environmental Engineering, James Worth Bagley College of Engineering, Mississippi State University, 2 Apr. 2010.
[16] J. M. Robertson, *Hydrodynamics in Theory and Application*. Englewood Cliffs, NJ: Prentice-Hall, 1965, pp. 548-559.
[17] http://www.emec.org.uk/marine-energy/wave-devices/.
[18] http://oceanlinx.com/.
[19] http://mysite.du.edu/~jcalvert/tech/fluids/turbine.htm#Impu.
[20] http://www.verdantpower.com/.
[21] A. Furukawa, S. Watanabe, K. Okuma, "Research on Darrieus type hydraulic turbine for extra low-head hydro power utilization," in *IOP Conf. Series: Earth and Environmental Science,* vol. 15, part 1, 2012.
[22] http://www.math.le.ac.uk/people/ag153/homepage/gorlovrevisedFish.pdf.
[23] http://www.engr.psu.edu/mtah/articles/vertical_waterwheel.htm.
[24] T. R. Akylas, C. C. Mei, "Forced dispersive waves along a narrow channel," *MIT Open Courseware - Modules on waves in Fluids,* Massachusetts Institute of Technology, ch. 6, 2001-2014.
[25] P. Chang, W. K. Melville, J. W. Miles, "On the evolution of a solitary wave in a gradually varying channel," *Journal of Fluid Mechanics*, vol. 95, part 3, pp. 401-414, 1979.
[26] http://oss.deltares.nl/documents/183920/185723/Delft3D-FLOW_User_Manual.pdf/.

K. D. R. Jagath-Kumara was born in Sri Lanka in 1963 and completed the primary and secondary school education in 1980. He received the BSc (1985), MEngSc (1992), and PhD (1997) degrees from the University of Peradeniya, Sri Lanka, the University of New South Wales, Australia, and the University of South Australia respectively. He was with the University of Oslo, Norway for two semesters in 1990.

Jagath was employed as an engineer from 1986-87 in the Ceylon Electricity Board and from 1987-89 in the Airports and Aviation Services (Sri Lanka) Ltd. He held research fellow positions at the University of South Australia from 1996-97 and at the University of Technology, Sydney, Australia in 1998. He was a lecturer in the Massey university, New Zealand from 2000-06. From 2006, he has been a senior lecturer in the University of Peradeniya, Sri Lanka. He has published 31 conference and journal articles since 1994. His research interests are on statistical signal processing, hybrid-ARQ, and energy systems.

Jagath is currently a corporate member of the Institution of Engineers, Sri Lanka. He has reviewed a large number of manuscripts for IEEE journals and conferences and for various other conferences.

D.D.Dias received the BSc (2007) and MSc (2011) degrees from the University of Peradeniya, Sri Lanka, and the University of Hokkaido, Japan, respectively. Further, he obtained a Diploma in Sustainability Science from the Center of Sustainability Science, Hokkaido University in 2010.

From 2009, he has been a lecturer in the University of Peradeniya, Sri Lanka. He has published 05 conference and one journal articles since 2011. His research interests are on the mathematical modeling of coastal morpho-dynamics, river bank stability, and sustainable energy.